



Contents lists available at ScienceDirect

Journal of Traditional and Complementary Medicine

journal homepage: <http://www.elsevier.com/locate/jtcme>

Moringa oleifera leaf extract induces osteogenic-like differentiation of human osteosarcoma SaOS2 cells

Mohammad Idreesh Khan ^a, Sahabjada Siddiqui ^{b, *}, Md. Abul Barkat ^c, Fahad Saad Alhodieb ^a, Fauzia Ashfaq ^d, Harshita Abul Barkat ^c, Abdulkareem A. Alanezi ^c, Md Arshad ^e

^a Department of Clinical Nutrition, College of Applied Health Sciences in Arrass, Qassim University, P.O. BOX:6666, Buraidah, 51452, Saudi Arabia

^b Department of Biotechnology, Era's Lucknow Medical College & Hospital, Era University, Lucknow, India

^c Department of Pharmaceutics, College of Pharmacy, University of Hafr Al-Batin, Al Jamiah, Hafr Al Batin, 39524, Saudi Arabia

^d Department of Clinical Nutrition, College of Applied Medical Sciences, Jazan University, Jazan, Saudi Arabia

^e Department of Zoology, Aligarh Muslim University, Aligarh, India

ARTICLE INFO

Article history:

Received 12 February 2022

Received in revised form

14 August 2022

Accepted 27 August 2022

Available online 2 September 2022

Keywords:

Moringa oleifera leaf

Cytotoxicity

Drug development

Osteoblast-like SaOS-2 cells

ABSTRACT

Introduction: *Moringa oleifera* is known as a 'natural nutrition of the tropics' because it provides vital nutritional supplements and a variety of pharmacological benefits. The focus of this study was to elucidate the dose dependent effects of *Moringa oleifera* leaf (MOL) extract on the growth of the human osteoblast-like osteosarcoma SaOS-2 cell line and primary osteoblast cells.

Methods: Trypan blue & tetrazolium assay, intracellular ROS generation, chromatin condensation, cell cycle analysis, alkaline phosphatase (ALP), mineralization, and osteogenic gene expression were tested on both treated and untreated osteosarcoma SaOS-2 cells.

Results: As revealed by cell viability assay, growth activity was observed at concentrations 25 and 50 µg/mL of MOL extract, whereas 100 and 200 µg/mL doses decreased the proliferation activity, resulting in ROS production and chromatin condensation. Cell cycle study revealed that MOL extract at 50 and 100 µg/mL concentrations arrested the cells in the G2/M phase. Low doses increased the ALP levels, mineralization, and expression of the bone morphogenetic protein 2 (BMP2) and runt-related transcription factor 2 (Runx2) genes in osteoblast-like SaOS-2 cells, however, high doses inhibited the proliferation properties of MOL extract. Through AutoDock Vina and iGEMDOCK 2.1, the interaction of active components of MOL, such as β-sitosterol, quercetin and kaempferol, with BMP2 and Runx2 proteins revealed a reasonable binding affinity. Moreover, these components did not show any Lipinski's rule of five violation and showed predictable pharmacokinetic properties.

Conclusion: The results of the biphasic dose-response of MOL extract on the growth activity of osteoblast-like SaOS-2 cells and *in silico* binding interface, may provide a therapeutic and/or preventive implication in prospective drug development.

© 2022 Center for Food and Biomolecules, National Taiwan University. Production and hosting by Elsevier Taiwan LLC. This is an open access article under the CC BY-NC-ND license (<http://creativecommons.org/licenses/by-nc-nd/4.0/>).

1. Introduction

Bone disorders such as arthritis, osteoporosis and osteosarcoma

* Corresponding author. Department of Biotechnology, Era's Lucknow Medical College & Hospital, Era University, Lucknow, 226003, India.

E-mail addresses: moi.khan@qu.edu.sa (M.I. Khan), sahabjada@erauniversity.in (S. Siddiqui).

Peer review under responsibility of The Center for Food and Biomolecules, National Taiwan University.

<https://doi.org/10.1016/j.jtcme.2022.08.006>

2225-4110/© 2022 Center for Food and Biomolecules, National Taiwan University. Production and hosting by Elsevier Taiwan LLC. This is an open access article under the CC BY-NC-ND license (<http://creativecommons.org/licenses/by-nc-nd/4.0/>).

are the worldwide problems of the human skeleton system. Osteoporosis is one of the global public health problems among bone disorders which represents major worldwide clinical, societal, and economical challenge. This is a chronic disease characterized by fragility in bone and fractures.¹ Over than 8.9 million people are suffering from osteoporosis, which causes an osteoporotic fracture every 3 s.² If the effects of population aging alone are accounted, the burden of osteoporosis and fragility fractures is predicted to rise dramatically over the next ten years.³ The aging population and higher life expectancy in Europe will cause osteoporosis to impact

List of abbreviations

MOL	Moringa oleifera leaf
MTT	3-(4,5-dimethylthiazol-2-yl)-2,5-diphenyl tetrazolium bromide
ALP	alkaline phosphatase
ROS	Reactive oxygen species
BMP2	Bone morphogenetic protein 2
Runx2	runt-related transcription factor 2
pNPP	p-nitrophenyl phosphate
HB	hydrogen bond
VDW	van der Waals forces
EI	electrostatic interactions
PASS	Prediction of activity spectra for substances
BAS	Bioactivity score
ADMET	Absorption, distribution, metabolism, excretion, and toxicity
BBB	blood -brain barrier
P-gp	P-glycoprotein

more than 30 million people by 2050.⁴

Several therapeutic methods for the treatment of bone disorders, such as chemotherapy and radiotherapy, have been developed; however, these conventional systems of therapies are known to have various complications such as nausea, anorexia, uncontrollable vomiting and diarrhea, dermatitis, electrolyte imbalance and bullous erythema multiforme, which reduce success rate in the majority of cases.⁵ Therefore, finding alternative therapies is crucial for resolving these issues and may be beneficial for those who have osteoporosis.

Plant extracts are well known indicative of their potential contribution to drug production because of their wide-ranging support and therapeutic applications.⁶ Medicinal plants and their ingredients are extremely important in the health-care systems of the world's population. For instance, date palm, figs, black cumin seeds, fruit and their active ingredients lutein, apigenin, β -sitosterol, *p*-hydroxybenzoic acid, *o*-coumaric acid, linoleic acid, palmitic acid, thymoquinone, dithymoquinone, and carvacrol have been found to be important in cancer and diabetes therapies, have shown antibacterial, antiviral, hepatoprotective, anti-hyperlipidemic, cardioprotective and antioxidant activities and are also helpful in pregnancy and delivery.⁷ In addition, *Gloriosa superba*, *Leea* species, *Centella asiatica*, *Echium amoenum*, *Withania somnifera* and *Nigella sativa* have been reported for potential antioxidant, antimicrobial, antidiarrhoeal, anticancer, analgesic, anthelmintic, anti-inflammatory, antipyretic, hepatoprotective, nephroprotective, neuroprotective activities.⁸

Among different medicinal plants, *Moringa oleifera* (MO) is the most commonly cultivated plant of the 'Moringaceae' family, which is known as 'natural nutrition of the tropics'. Interestingly, nearly all parts of the MO plant such as leaves, roots, seed, bark, fruit, flowers and immature pods contain important nutritional supplements with a variety of medicinal properties.^{9–11} Many essential components *viz.* alkaloids, flavonoids, terpenoids, steroidal aglycones, tannins and reducing sugars, can be found in the leaves, barks, roots, seeds, flowers, and immature pods of the MO plant.¹² Various parts of this multipurpose tree have been credited with several beneficial and medicinal properties which include anti-fibrotic, anti-inflammatory, anti-microbial, anti-hyperglycemic, antioxidant, anti-tumor, and anti-cancer activities.¹⁰ An earlier study has proven the osteogenic activity of MO and *Cissus quadrangularis* in mandibular fracture clinically.¹³

Moringa oleifera leaf (MOL) is the store house of vital components *viz.* carotenoids, flavonoids, tocopherols, folate, phenolic acids, polyunsaturated fatty acids and various minerals.¹⁴ Earlier studies have also shown that MOL contains the bioactive components *viz.* β -sitosterol, quercetin and kaempferol.^{15,16} Some previous researchers have shown that many dietary phytoestrogens such as genistein, daidzein, biochanin A, glabrene isoflavene, isoliquiritigenin, kaempferol, resveratrol and other phytochemicals demonstrated biphasic hormetic like dose-response effects.^{17–20} However, to date, no scientific study has evaluated the dose-dependent biphasic effects of *moringa oleifera*. Therefore, we hypothesized that MOL extract might have hormetic-like dose-dependent biphasic effects on cell growth of human osteoblast-like SaOS-2 cell line.

In the present study, an *in vitro* dose-response potential of MOL extract against SaOS-2, a human osteoblast-like cell line was investigated using cell viability assay, analysis of ROS, nuclear apoptosis, cell cycle, ALP analysis, mineralization, and osteoblastic bone morphogenetic protein 2 (BMP2) and runt-related transcription factor 2 (Runx2) gene expression. Moreover, an *in-silico* structure-based virtual screening technique was used to determine MO leaf bioactive components β -sitosterol, quercetin and kaempferol with BMP2 and Runx2 proteins. The results on the biphasic dose-response of MOL extract may have a potential therapeutic or preventive implication in drug development.

2. Materials and methods

2.1. Reagents, chemicals, and plant materials

Entire cell culture media, supplements and all chemicals were purchased from Sigma-Aldrich (St. Louis, MO, USA) and Hi-media (Mumbai, India). Fresh and spotless leaves of MO plant were collected in the month of August nearby Lucknow, India, and was scientifically identified in the herbarium of Pharmacognosy and Phytochemistry Department at Integral University, Lucknow, India (file no. IU/PHAR/HRB/14/07). Healthy leaves of MO weighing 450 g were washed with sterile water, air-dried for a week and then grinded into a coarse powder. Plant materials were soaked in 95% ethanol in 1:4 ratio (w/v) at 25 °C for 3 days to extract the soluble components. The supernatant was filtered with Whatman No.1 filter paper and then was concentrated at 40–45 °C in water bath. The obtained semi-solid paste (approx. 10% yield) was stored at room temperature and used for experimental purposes.

2.2. Osteoblast-like cell line, primary osteoblasts and their culture

Human osteoblast SaOS-2 cell line (passage no. 24) was procured from cell repository at National Centre for Cell Sciences, Pune, India. SaOS-2 cell line was grown in McCoy's 5A medium (Hi-media Mumbai, India) with 2.0 mM L-glutamine, 1.0% penicillin and streptomycin solution supplemented with 0.5 g/L NaHCO₃ and 10% Fetal bovine serum (Hi-media Mumbai, India). Primary osteoblasts were isolated from rat pups calvaria as per the previous standard method and maintained in alpha-MEM containing 10% FBS and 1% penicillin/streptomycin solution in a CO₂ incubator at 37 °C, 5% CO₂ with humidified air.¹⁹ Institutional Animal Ethics Committee approval number of the animal study is IAEC/ELMCH/1/21/-2.

2.3. Trypan blue staining and MTT assay

The percent cells viability of SaOS-2 cell line at 25, 50, 100 and 200 μ g/mL concentrations of MOL was evaluated at different time periods 24, 48 and 72 h using trypan blue staining assay. Based on growth pattern of cells, SaOS2 cell line and primary osteoblast cells

was evaluated further for cell viability at 48 h by MTT dye.²¹ In each well of a 96-well culture plate, approximately 1×10^4 cells were seeded in 0.1 mL of growth medium. The stock of MOL extract was prepared in culture media and diluted to the desired concentrations in the medium (25, 50, 100 and 200 $\mu\text{g}/\text{mL}$) and applied to each well. After 48 h of treatment, microphotograph was captured using a microscopy of trinocular inverted phase-contrast (Nikon ECLIPSE TS100, Japan) and a microplate reader (BIORAD-PW41, California, USA) was used to measure the absorbance at 540 nm.

2.4. DCFDA staining dye for ROS activity

To determine the impact of low and high dose of MOL on reactive oxygen species (ROS) development in SaOS-2 cells, fluorescence imaging microscope and multiwell plate reader techniques were used.²² In a 96-well black bottom culture plate, SaOS-2 cells (1×10^4 per well) were cultured and treated with different concentrations of MOL extract for 24 h, as 24 h time period was enough for ROS generation treated cells. The cells were incubated with DCFH-DA (10 mM) dye and fluorescence intensity was determined using a multiwell plate reader (BioTek's Synergy H1 Hybrid Multi-Mode Microplate Reader, VT, USA). Results were expressed as a percentage of the fluorescence intensity relative to control groups. For Imaging of ROS intensity, cells were incubated with MOL extract in 24-well plate for 24 h and images were captured after DCFHDA staining under an inverted fluorescence microscope (Zeiss AxioVert 135, USA).

2.5. Chromatin condensation

Using the nuclear fluorescent dye DAPI, the apoptotic effect of MOL at various concentrations was investigated.²³ After 48 h of incubation with MOL extract, the cells were fixed in 4% paraformaldehyde and stained with DAPI dye. The photos were taken with a fluorescent inverted microscope after staining. Apoptotic cells were described as those with condensed nuclei.

2.6. Cell cycle phase distribution

Flow cytometric analysis was used to examine the relationship between cell cycle phase and cellular DNA material. SaOS-2 cells were seeded at a density of 1×10^6 cells/mL in a 6-well plate and treated with two effective doses of MOL extract, 50 $\mu\text{g}/\text{mL}$ (proliferative dose) and 100 $\mu\text{g}/\text{mL}$ (cytotoxic dose), for 48 h and were incubated in a 5% CO₂ incubator at 37 °C.²⁴ The stained cells with propidium iodide (PI) dye were used to test the PI fluorescence of individual nuclei using a flow cytometer (BD FACS Calibur, Becton Dickinson, USA). The Cell Quest Pro V3.2.1 programme (Becton Dickinson, USA) was used to analyse the data.

2.7. ALP quantification assay

In an ALP assay, the *p*-nitrophenyl phosphate (pNPP) substrate is hydrolyzed into a yellow-colored product which was measured as per the previous method.²¹ Approximately, 2×10^3 cells of SaOS2/well per 100 μL media was seeded in 96-well plate using McCoy's 5A medium containing 10% FBS, 50 $\mu\text{g}/\text{mL}$ ascorbic acid and 10 mM β -glycerophosphate (differentiation medium) overnight. The cells were then incubated for 48 h with concentrations of MOL extract of 25, 50, 100, and 200 $\mu\text{g}/\text{mL}$. An inverted phase contrast microscope was used to capture the creation of colour images and the absorbance was estimated at 405 nm with the help of an ELISA reader (BIORAD-PW41, California, USA).

2.8. Mineralization assay

Calcium contents in SaOS-2 cells were measured using Alizarin Red S stain as per the method reported previously.²¹ In a 12-well culture plate (Himedia, India), 2×10^4 cells/well were seeded in 500 μL differentiation medium containing 10^{-7} M dexamethasone. MOL extract was given to the cells for 21 days, and the medium was changed every other day. The cells were fixed in paraformaldehyde solution and stained with 40 mM Alizarin Red-S. Calcified nodules with a bright red colour were captured under inverted phase contrast microscopy. To determine the quantitative value, a 100 mM cetylpyridinium chloride solution was applied to each well for 1 h to solubilize and release the calcium-bound alizarin red into solution in each well. Every well's supernatant was transferred in triplicate to a 96-well plate, and the absorbance was measured at 570 nm using a microplate reader (BIORAD-PW41, California, USA).

2.9. Real-time quantitative PCR (qPCR) analysis

SaOS-2 cells were treated with MOL extract at various concentrations in T-25 cm² flask for 48 h and the expression analysis of BMP2 and Runx2 gene was performed using an earlier method.²² Following the manufacturer's instructions, total RNA was isolated from treated and untreated cells using the RNAiso Plus reagent. The Revert Aid First Strand cDNA Synthesis Kit (Thermo Scientific, Waltham, MA, USA) was used to synthesize cDNA from 1 μg of isolated RNA. A spectrophotometer (Thermo 2000C, USA) was used to determine the concentration of cDNA, and 12.5 ng/ μL cDNA was used for qPCR analysis. The LightCycler 480 SYBR Green I kit (Roche, Mannheim, Germany) was used to conduct real-time PCR analysis in a light cycler PCR system (Light Cycler 480, Roche, Mannheim, Germany). A standard curve of treated and untreated cells of known template concentration was generated for absolute quantification, and the concentration of the unknown sample was calculated by interpolating its PCR signal (cycle threshold) into the standard curve. Sequence of Runx2 gene primer pair was: Forward: 5'-CACAGAGCTATTAAGTGACAGTG-3'; Reverse: 5'-AACAAAC-TAGGTTTAGAGTCATCAAGC-3'; Sequence of BMP-2 gene primer pairs was: Forward: 5'-ATGGATTCTGGTGGAAAGTG-3', Reverse: 5'-GTGGAGTTCAGATGATCAGC-3'.

2.10. Molecular docking study

AutoDock Vina and iGEMDOCK V2.1 were used to investigate the binding relationship of β -sitosterol, quercetin and kaempferol with BMP2 and Runx2 protein. The 3D structure of ligand was obtained from the PubChem database, and energy minimization was carried out using ChemBio3D Ultra 14.0, with Force Field type MM2 and saved in.pdb format. The BMP2 and Runx2 proteins' 3-D crystal structure was downloaded in.pdb format from the RCSB-Protein Data Bank. Based on binding energy, AutoDock Vina was used to perform docking analysis, producing 9 conformations of the ligand-protein complex. Accelrys Biovia Discovery Studio version 2017 R2 was used to visualise the conformations with the lowest binding energy. The genetic algorithm parameters of the docking procedure were set using iGEMDOCK V2.1 as follows: population size = 200, generations = 70, and number of solutions = 2. The best match was chosen displaying total binding energy, which is the aggregate of hydrogen bond (HB), van der Waals forces (VDW), and electrostatic interactions (EI) energy. Accelrys Biovia Discovery Studio 2017 R2 was used to imagine the optimal fit of the ligand-protein interaction.²⁵

2.11. PASS program

Based on the structure-activity relationship, the Prediction of Activity Spectra for Substances (PASS) study predicts biological and pharmacological activities of compounds as well as their mechanism of action.²⁶ The following parameters were used to conduct the PASS analysis in this study:

2.11.1. Lipinski's rule of five

Lipinski's rule of five was used to assess the drug-likeness of β -sitosterol, quercetin and kaempferol active constituents.²⁷ The Molinspiration online tool was used to calculate the various physicochemical properties as described in Table 3.

2.11.2. Drug-likeness and toxicity potential study

Toxicity risk assessment analysis offers preliminary information of phytochemical's side effects that can be used in lead discovery and development. Prediction of various properties of phytochemicals is a crucial step in the early stages of drug development. Druglikeness, mutagenic, tumorigenic, reproductive, and irritant effects of drug-toxicity risk parameters were analysed using OSIRIS Data Warrior V5.2.1 online software.²⁶

2.12. Bioactivity score (BAS) prediction

BAS values indicate a compound's overall potential as a drug candidate. Molinspiration cheminformatics (<https://www.molinspiration.com/cgi-bin/properties>) was used to predict the drug scores of phytoconstituents against a variety of human receptors, including GPCRs, ion channels, kinases, nuclear receptors, proteases, and enzymes. As a rule of thumb, the higher the

bioactivity score, the more likely the compound is to be active.²⁸

2.13. Pharmacokinetics study

The pharmacokinetic properties of active components in MOL, such as absorption, distribution, metabolism, excretion, and toxicity (ADMET), were predicted using the online SwissADME program. A number of pharmacokinetic properties including blood-brain barrier (BBB), skin permeability (Log Kp), and metabolism as a P-glycoprotein (P-gp) substrate, cytochrome P450 inhibitor, as well as their lipophilicity were investigated.²⁹

2.14. Statistical analysis

The results were expressed in triplicates as the means \pm SEM with statistical significance calculated using ANOVA and Dunnett's multiple comparison tests. Statistical significance was defined as a probability value of $p < 0.05$. The programme GraphPad Prism (Version 5.1) was used to perform all of the analyses.

3. Results

3.1. Microscopic observation and cell viability analysis of SaOS-2 cells

Osteoblast-like SaOS-2 cells were treated with different concentration of MOL extract at different time periods and trypan blue staining was used to detect the cell growth kinetic. As shown in Fig. 1A, doses 25 and 50 $\mu\text{g/mL}$ of MOL extract increased the viable cells (trypan blue dye excluding) number at 24, 48 and 72 h of incubation, while 100 and 200 $\mu\text{g/mL}$ of MOL extract reduced the

Table 1

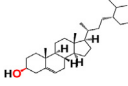
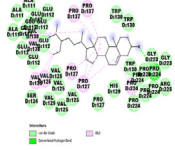
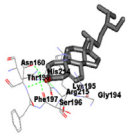
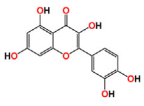
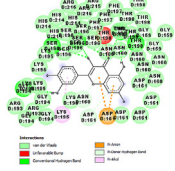
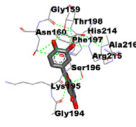
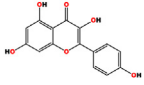
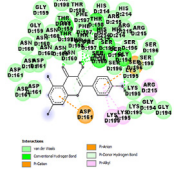
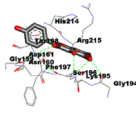
Docking interactions of Beta-sitosterol, quercetin and kaempferol with human Bone Morphogenetic Protein-2 (BMP2, PDB ID: 3BMP; Homo 2-mer - A2) using AutoDock 4.2 and AutoDock Vina. Ligand-protein complex is represented by the 2-D line model in AutoDock Vina and 3-D stick model was used in iGEMDOCK 2.1 analyses colored by- H = White, C = Grey, N = Blue, O = Red, S = Yellow, Pink = other elements. The hydrogen and pi-alkyl bond interactions are shown as green and magenta broken lines, respectively.

AutoDock Vina		iGEMDOCK v2.1							
Ligand with MF, MW and PubChem CID	BE (kcal/mol)	Interacting amino acids	2-D Structure	T.E. (kcal/mol)	VDW	HB	EI	Interacting amino acids	3-D Structure
Beta-sitosterol MF: C ₂₉ H ₅₀ O MW: 414.7 PubChem CID:222284	-7.8	Trp28, Trp31, Asp30, Glu96, Glu94, Asp93, Met89, Leu92, Met106, Tyr103		-77.44	-70.67	-6.77	0	Lys73, Ser72, Ile74, Pro75, Lys76, Cys78, Glu46, Cys79, Gly45, His44	
Quercetin PubChem CID: 5280343 MF: C ₁₅ H ₁₀ O ₇ MW: 302.23 g/mol	-6.6	Tyr91, Leu92, Glu96, Asp93, Glu94, Trp31, Leu92, Asp93, Trp28		-92.07	-63.37	-28.70	0	Asn68, Pro75, Lys76, Ala77, Cys78, Cys47, Cys79, Glu46, Gly45	
Kaempferol PubChem CID: 5280863 MF: C ₁₅ H ₁₀ O ₆ MW: 286.24 g/mol	-6.3	Trp28, Trp31, Asp30, Asp93, Glu94, Glu96, Asp93, Leu92		-79.99	-56.07	-23.92	0	Lys11, Leu10, Glu46, Gly45, His44, Cys79, Cys78, Ala77, Lys76	

Abbreviation: MW, molecular weight; MF, molecular formula, BE, binding energy; TE, total energy; VDW, van der Waals interaction; HB, hydrogen bond; EI, electrostatic interaction.

Table 2

Docking interactions of Beta-sitosterol, quercetin and kaempferol with executioner Runt-related transcription factor 2 (Runx2; PDB ID: 6VGE; Hetero 3-mer - A1B1C1) using AutoDock 4.2 and AutoDock Vina. Ligand-protein complex is represented by the 2-D line model in AutoDock Vina and 3-D stick model was used in iGEMDOCK 2.1 analyses colored by- H = White, C = Grey, N = Blue, O = Red, S = Yellow, Pink = other elements. The hydrogen and pi-alkyl bond interactions are shown as green and magenta broken lines, respectively.

AutoDock Vina			iGEMDOCK v2.						
Ligand with MF, MW, Molecular Structure and PubChem CID	BE (kcal/mol)	Interacting amino acids	2-D Structure	T.E. (kcal/mol)	VDW	HB	EI	Interacting amino acids	3-D Structure
Beta-sitosterol MF: C ₂₉ H ₅₀ O MW: 414.7 PubChem CID:222284 	-6.6	Ala111, Glu112, Val125, Ser124, Pro127, His129, Pro224, Trp130, Arg225, Pro224, Gly223		-73.93	-63.52	-10.41	0	Asn160, His214, Thr198, Lys195, Arg215, Phe197, Ser196, Gly194	
Quercetin PubChem CID: 5280343 MF: C ₁₅ H ₁₀ O ₇ MW: 302.23 g/mol Chemical Class: Polyphenolic Flavonoid 	-6.1	Thr198, Gly159, Asn160, Asp161, Thr198, Asn160, Phe197, Arg215, Ser196, His214, Lys195, Gly194, Arg193, Gly194		-91.42	-50.57	-40.85	0	Gly159, Thr198, His214, Phe197, Asn160, Ala216, Arg215, Ser196, Lys195, Gly194	
Kaempferol PubChem CID: 5280863 MF: C ₁₅ H ₁₀ O ₆ MW: 286.24 g/mol Chemical Class: Tetrahydroxyflavone 	-6.2	Thr198, Gly159, Phe197, His214, Arg215, Ser196, Asn160, Gly194, Lys195, Lys196, Arg216, Asp161, Asn160, Gly159, Thr198, Phe197, Thr198		-86.83	-67.90	18.93	0	His214, Arg215, Thr198, Asp161, Gly159, Asn160, Phe197, Ser196, Lys195, Gly194	

Abbreviation: MW, molecular weight; MF, molecular formula, BE, binding energy; TE, total energy; VDW, van der Waals interaction; HB, hydrogen bond; EI, electrostatic interaction.

Table 3

PASS analysis of most active phytoconstituents.

Lipinski's rule of 5 parameters (Physiochemical parameters)										
S. No.	Phytoconstituent % Absorption (>50%) ^a	Topological Polar Surface Area (Å) ^b (160 Å)	MW (<500)	c logP (<5) ^c	Heavy atom count (n atoms)	Hydrogen Bond Donors (nOHNH) (≤5)	Hydrogen Bond Acceptors (nON) (≤10)	Number of Rotatable bonds (≤10)	Lipinski's violation	
1.	Beta-sitosterol	102.02	20.23	414.72	8.62	30	1	1	6	1
2.	Quercetin	63.68	131.35	131.35	1.68	22	5	7	1	0
3.	Kaempferol	70.66	111.12	286.24	2.17	21	4	6	1	0

Note.

^a Percentage absorption was calculated as: % Absorption = 109- [0.345xTopological Polar Surface Area].

^b Topological polar surface area (defined as a sum of surfaces of polar atoms in a molecule).

^c Logarithm of compound partition coefficient between n-octanol and water.

viable cell number both dose and time dependant manner. Although, MOL extract increased the necrotic (trypan blue positive) cells both dose and time dependant manner as compared to control. Based on the trypan blue cell growth data, 48 incubation period was selected for further cell viability analysis of SaOS-2 cells at different doses of MOL extract using MTT mitochondrial assay. Fig. 1B and C show the comparative cell morphology and cell viability of untreated and treated osteoblast SaOS-2 cells with MOL extract, respectively. Cells treated with 25 and 50 µg/mL of MOL extract changed the morphology of the cell with a more elongated

shape showing cell proliferation. However, MOL extract at concentrations of 100 and 200 µg/mL distorted to an almost spherical shape, inhibited cell proliferation, and compromised membrane integrity. In comparison to the control, the concentrations of 25 and 50 µg/mL of MOL extract increased the viability of the cells by 119.5 and 151.82%, respectively, while, 100 and 200 µg/mL extract reduced the cell growth to 96.34 and 71.86%. The results of primary osteoblasts were consistent with results of osteosarcoma cell line (Fig. 1D and E).

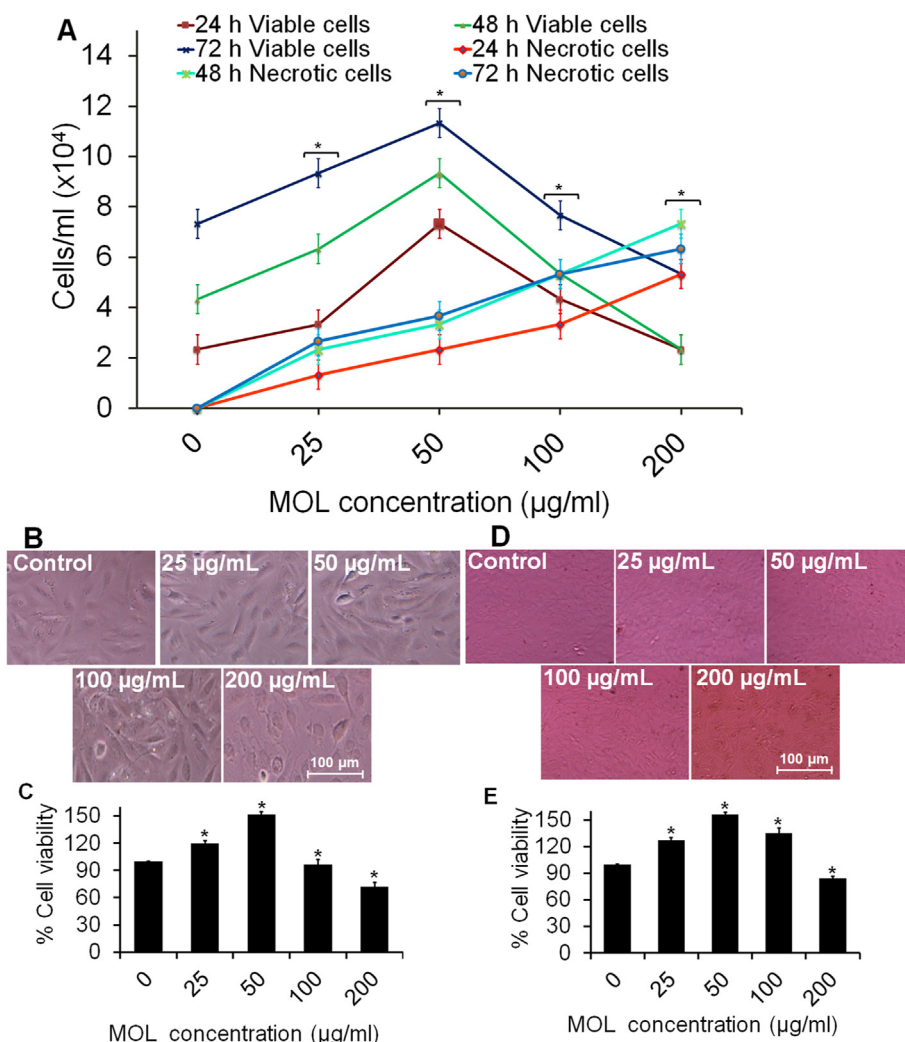


Fig. 1. Trypan blue and MTT assay of MOL extract against human osteosarcoma SaOS-2 cell line and normal primary rat calvaria osteoblasts (A) Growth curve of viable (trypan blue excluding) and necrotic (trypan blue positive) cells $\times 10^4$ /ml of SaOS-2 cell line treated at various concentrations of MOL extract at 24, 48 and 72 h periods. (B) Morphological variation of untreated and treated SaOS-2 cells at various concentrations of MOL extract, Bar = 100 μ m (C) As stated in the experimental section, the percent cell viability of SaOS-2 cells was calculated at 48 h through MTT assay (D) Morphological variation of primary osteoblasts at various concentrations of MOL extract, Bar = 100 μ m (E) the percent cell viability of primary osteoblasts cells at 48 h through MTT assay. The results are expressed as the means \pm SEM of at least three independent experiments. * $p < 0.05$ as compared with their respective control.

3.2. Effects of MOL extract on ROS generation, nuclear apoptosis and cell cycle arrest

As evident from fluorescent microscopic images (Fig. 2A), with increasing concentrations of MO extract, the intensity of ROS was decreased slightly while the native morphology of the cells was preserved. However, 100 and 200 μ g/mL of MOL extract considerably induced the ROS levels in cells with deformed morphology. The quantitative data were consistent with the findings of fluorescent microscopic images (Fig. 2B). As observed from the photomicrograph (Fig. 2C), the exposure of SaOS-2 cells at 100 and 200 μ g/mL of MOL induced apoptosis in the cells where the dye's permeability was increased. In a cell cycle study, SaOS-2 cell was treated at a proliferative dose and other at a toxic dose viz. 50 and 100 μ g/mL of MOL for 48 h and various stages of the cell cycle was detected. The control group had a normal distribution of the cell cycle, as seen in the results (Fig. 2D). After treatment with MOL at 50 and 100 μ g/mL, a large number of cells were accumulated in the apoptotic phase (subG0), with a considerable number accumulated in G2/M phase. Results revealed that both 50 and 100 μ g/mL of the

plant extract resulted in extensive accumulation of cell density in the G2/M phase while MOL at 100 μ g/mL suppressed its own promoting effect in S phase and caused cell apoptosis.

3.3. Effect of MOL on differentiation, mineralization and Runx2/BMP-2 gene expression

The qualitative and quantitative data of ALP analysis showed that the concentration 25 and 50 μ g/mL MOL extract stimulated the rate of osteoblast cell differentiation by increasing ALP stain and its level. However, 100 and 200 μ g/mL MOL extract decreased the ALP level (Fig. 3A and B). The concentrations 25 and 50 μ g/mL of MOL increased mineralized nodules in cultured osteoblast, suggesting osteogenic effect ($p < 0.05$) when compared with control. However, concentrations 100 and 200 μ g/mL of MOL extract turned to decrease the level of mineralization (Fig. 3C and D). As is shown in Fig. 3E and F, concentrations 25 and 50 μ g/mL of MOL extract elevated the expression profile of BMP2 and Runx2 genes while the expression level of both genes was decreased at 100 and 200 μ g/mL of the plant extract.

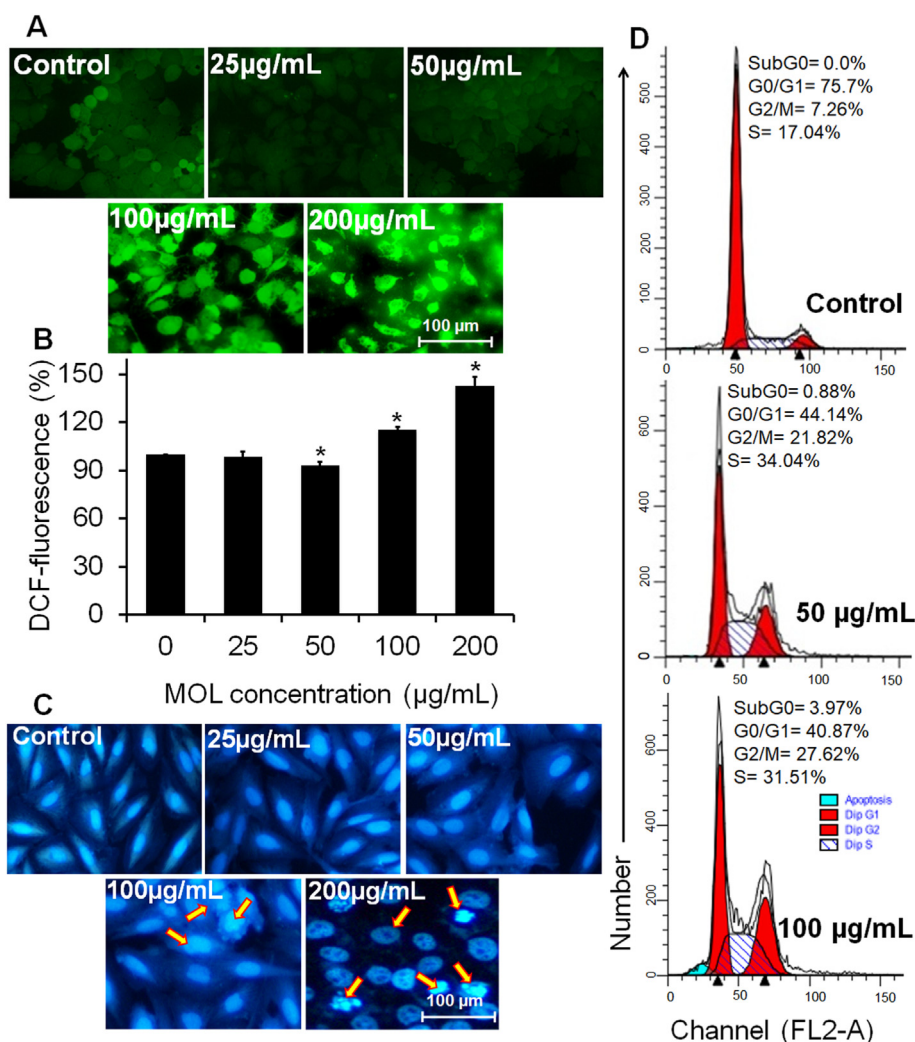


Fig. 2. Effect of MOL extract on ALP level, mineralization and expression analysis of BMP2 and Runx2 genes in SaOS-2 cells (A) Photomicrographs showing the ALP stain in treated and untreated SaOS-2 cells at various concentrations (25–200 µg/mL) of MOL extract at 48 h, Bar = 100 µM (B) Quantitative data of ALP level represented as ALP activity relative to control which was measured with a colorimetric assay using p-nitrophenyl phosphate disodium as a substrate (C) Photomicrographs showing mineralized nodules formation of SaOS-2 cells stained with alizarin red-S, Bar = 100 µm (D) Quantitative estimation of the formation of the mineralized nodule which is expressed as OD (E & F) Graph showing the qPCR analysis of BMP2 and Runx2 gene expression. Data are shown as mean ± SEM of three independent experiments. * $p < 0.05$ as compared to control.

3.4. Molecular docking analysis

The binding relationship of β -sitosterol, quercetin and kaempferol with BMP2 and Runx-2 proteins was investigated through AutoDock Vina and iGEMDOCK 2.1. The obtained best pose of interaction was visualized using Accelrys Biovia Discovery Studio. Molecular docking analyzes by AutoDOck Vina revealed that β -sitosterol, quercetin, and kaempferol had potent binding interactions with BMP2 protein, with binding energies of -7.8 , -6.6 , and -6.6 kcal/mol, respectively (Table 1). When analysed using Autodock Vina, the ligands β -sitosterol, quercetin, and kaempferol exhibited potent binding interactions with Runx2 protein, with binding energies of -6.6 , -6.1 , and -6.2 kcal/mol, respectively. This interaction was further confirmed from analysis using iGEMDOCK 2.1 software. The molecular interactions represent interacting amino acid residues in binding pockets has also been shown in Tables 1 and 2.

3.5. PASS analysis of active constituents

Table 3 displays the physicochemical properties of MOL

ingredients according to Lipinski's rule of 5. Lipinski's violation should not be more than one for an orally active compound. Interestingly, β -sitosterol had only one violation of Lipinski's rule of five, whereas quercetin and kaempferol did not. The logPc value indicates that phytochemicals are well absorbed or permeated through the intestinal wall. Except for β -sitosterol, both quercetin and kaempferol exhibited this property.

3.6. Druglikeness and toxicity calculation

Table 4 depicts the drug-likeness and toxicity potential of active components using the OSIRIS Data Warrior V5.2.1 software. According to the data, all of the ingredients are safe to use and will not cause any toxicity. Quercetin was found to be mutagenic and tumorigenic, whereas kaempferol was found to be highly mutagenic.

3.7. Bioactivity scores (BAS) analysis of drug targets

Molecules with a BAS score of >0.00 is thought to be biologically active, while one with a BAS score of -0.50 to 0.00 is thought to be

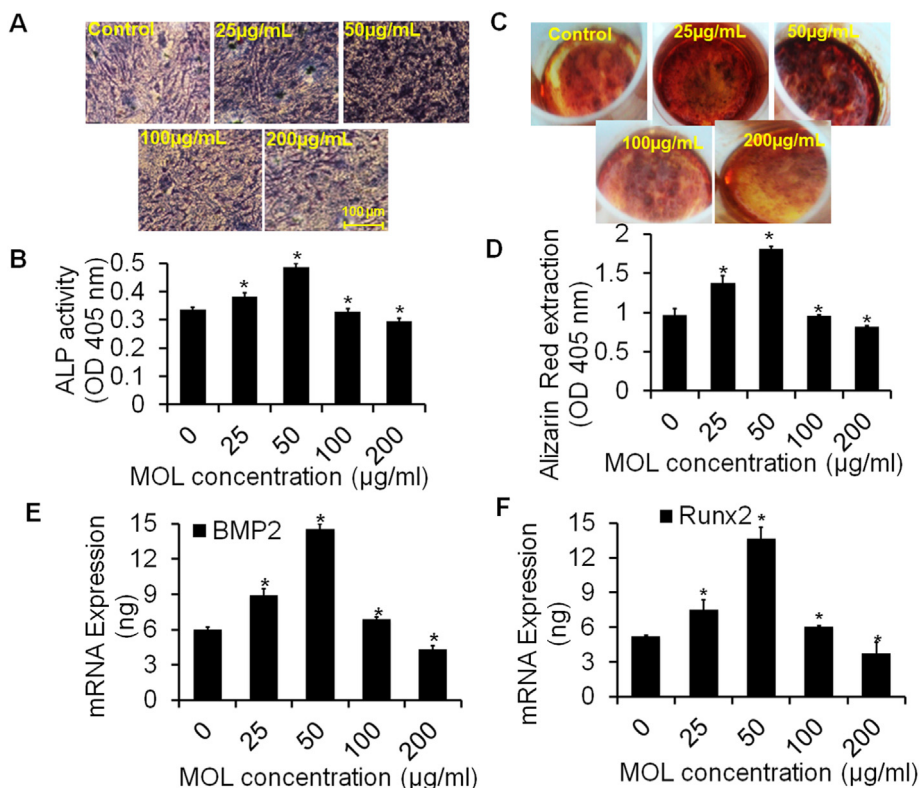


Fig. 3. Effect of MOL extract on ROS generation, nuclear condensation and cell cycle progression of SaOS-2 cells (A) Photomicrograph stained with DCFDA dye displaying intracellular ROS production induced by MOL extract at various concentrations (B) Measurement of ROS level is expressed as the percentage of fluorescence intensity relative to the control (C) Fluorescence microscopy images of SaOS-2 cells stained with DAPI showing nuclear condensation under an inverted fluorescence microscope (D) Representative photomicrographs displays the apoptosis and phase distribution of cell population at 50 and 100 µg/mL of MO extract after 48 h. The results are expressed as means ± SEM of at least three independent experiments, *p < 0.05, as compared to control. Scale bar 100 = µm.

Table 4
Druglikeness and toxicity calculation of MOL phytoconstituents.

S. No.	Compounds Name	Druglikeness	Mutant	Tumurogenic	Reproductive effective	Irritant
1.	Beta-sitosterol	-4.475	None	None	None	None
2.	Quercetin	-0.82832	High	High	None	None
3.	Kaemferol	-0.82832	High	None	None	None

moderately active, and one with a BAS score of -0.50 is thought to be inactive. Surprisingly, all of the ingredients were found to be biologically active and/or moderately active. As a result, β-sitosterol, quercetin, and kaempferol are thought to exert physiological effects via a variety of mechanisms, including interactions with ion channel modulators, GPCR ligands, nuclear receptor ligands, and protease and kinase enzyme inhibitors.

3.8. ADMET (absorption, distribution, metabolism, excretion, and toxicity) properties

The pharmacokinetic properties of β-sitosterol, quercetin, and

kaempferol were calculated using online SwissADME software (Table 6). The lower the log Kp, the less permeant the molecule is to the skin²⁸. The calculated LogKp value showed that β-sitosterol is more skin permeant than quercetin and kaempferol. Lipophilicity is an important drug parameter that influences its activity in the human body. The compound's Log P value indicates the drug's ability to reach the target tissue in the body. Because their Log P is greater than or equal to one, all of the ingredients are lipophilic. As a result, all of the ingredients are lipophilic and absorb well across the skin. None of the components were permeable to the blood-brain barrier (BBB). Furthermore, none of the components serve as P-glycoprotein substrates (P-gp). P-gp is an ATP-dependent

Table 5
Bioactivity scores of MOL active ingredients.

S. No.	Bioactivity score parameter						
	Ligand	GPCR ligand	Ion channel modulator	Kinase inhibitor	Nuclear receptor ligand	Protease inhibitor	Enzyme inhibitor
1.	Beta-sitosterol	0.14	0.04	-0.50	0.73	0.07	0.51
2.	Quercetin	-0.06	-0.19	0.28	0.36	-0.25	0.28
3.	Kaempferol	-0.10	-0.21	0.21	0.32	-0.27	0.26

Table 6
ADMET properties calculated by swissADME.

S. No.	Components	Lipophilicity (Consensus Log Po/w)	BBB permeant	P-gp substrate	CYP1A2 inhibitor	CYP2C19 inhibitor	CYP2C9 inhibitor	CYP2D6 inhibitor	CYP3A4 inhibitor	Log Kp (skin permeability coefficient)
1.	Beta-sitosterol	7.19	No	No	No	No	No	No	No	–2.20 cm/s
2.	Quercetin	1.23	No	No	Yes	No	No	Yes	Yes	–7.05 cm/s
3.	Kaempferol	1.58	No	No	Yes	No	No	Yes	Yes	–6.70 cm/s

protein pump that removes drugs from the human body, reducing phytomolecule pharmacokinetic efficacy. As a result, the active ingredients of MOL may remain in the cells and confirm their intracellular pharmacological role. Cytochromes P450 (CYPs) are metabolic enzymes involved in drug metabolism; if one drug inhibits the CYPs-mediated metabolism of another, the second drug may accumulate inside the body and cause toxic effects. In this study, none of the MOL components were found to be acting as inhibitors of CYPs, except quercetin and kaempferol for CYP1A2, CYP2D6 and CYP3A4.

4. Discussion

The present study evidenced for the cell's growth potential of MOL extract against osteoblast cell line by providing the osteogenic effects as well as cytotoxic potential depending upon dose. Bone formation process is called osteogenesis or ossification which includes three stages of development: 1) cell differentiation, called proliferation 2) maturation of matrix, and 3) mineralization.³⁰ A fine balance between bone formation and bone resorption is required for healthy bone tissue, and this will be the first step in osteoporosis treatment. To investigate the effect of MOL extract on bone cells metabolism, we employed a cell culture system with SaOS-2 of human osteoblast-like osteosarcoma cells. This study supported the results showing cells exposed to low concentration of MO extract causes osteoblast differentiation as a function of dose through morphological changes and an increase in the number of cells.³¹ Low doses of MO leaf extract improved cell proliferation by increasing the number of bone cells and their compactness, as shown in Fig. 1 B, whereas, high doses reduced the bone cells number and their compactness. One of the biochemical approaches is to measure alkaline phosphatase activity quantitatively that offer information about early cell differentiation of osteoblast.³² Naturally occurring flavone β -sitosterol has shown a stimulatory effect on alkaline phosphatase activity in osteoblast cells.³³ More interestingly, a previous study has supported our results that MOL extract ranging from 0 to 50 $\mu\text{g}/\text{mL}$ have less significant activity on liver cancer HepG2 cells proliferation and its apoptosis, however, doses ranging from 100 to 300 $\mu\text{g}/\text{mL}$ have prominent effects on HepG2 cancer cells death.³⁴

Further, to check the cytotoxic effects of higher doses of MO leaves extract, both treated and untreated osteosarcoma SaOS2 cells were tested for nuclear condensation, ROS generation and cell cycle arrest. Result of DAPI fluorescence stain showed that high doses of MOL induced the apoptosis of the cell with nuclear fragmentation, while DCFHDA stain revealed the ROS-mediated cell death in osteosarcoma cells at higher concentrations of MOL extract. In a previous study, luteolin, a flavonoid, showed a protective effect against hyperglycemic induced ROS generation in MG-63 cells, however, high concentrations of luteolin demonstrated osteoblast cell death in normal and high-glucose states via increasing ROS and decreasing alkaline phosphatase activity.³⁵ In another study, quercetin, a flavonoid, induced growth inhibition of 143B osteosarcoma cell line and arrested the cell cycle in G2/M phase.³⁶ Cell cycle data revealed that doses 50 and 100 $\mu\text{g}/\text{mL}$ of

MOL extract arrested the cells in the G2/M phase. More importantly, low dose of MOL exhibited the promoting effect by arresting the cells in S phase while decreasing the promoting effect at high dose by preventing them from entering the S phase and thus decrease the cell proliferation (Fig. 2D). In a similar study, low doses of aspirin have induced cell cycle arrest at the G0/G1 phase and decreases the S phase by preventing them from entering the S phase and thus decreasing proliferation.³⁷

Mineralized nodules are phenotypic markers for osteoblasts that identify the final stages of differentiation, which take place after cell proliferation and matrix maturation.³⁸ As a result, it takes at least 21 days for calcium nodules formation and therefore, mineralization assay was performed after 21 days of incubation. In our study, low doses of MO leaf extract induced the calcium nodule formation but high doses reversed the process of mineralization (Fig. 3C and 3D). BMP2 is one of the most powerful cytokines that promote differentiation of mesenchymal cells into osteoblasts *in vitro* and induce bone formation *in vivo*. BMP2 exhibits this osteogenic action by activating Smad signaling and by regulating transcription of osteogenic genes such as Runx2, type I collagen, osteocalcin, and bone sialoprotein³⁹. Runx2 is a key transcription factor initiating early osteogenesis as the master gene of bone formation, late mineralization, and expression of major bone matrix genes during the early stages of osteoblast differentiation.⁴⁰ In our study, low doses of MO leaves extract induced the osteogenic genes BMP2 and Runx2 expression, whereas, high doses reduced the expression level of both genes. This study suggested the hormetic-like biphasic dose-response effects of MO leaves on the bone cells proliferation and differentiation. A previous study has reported that nutraceuticals curcumin and carnolic acid synergistically promoted osteogenesis in cultured murine 7F2 osteoblast cells and alleviated microgravity-induced inhibition of osteogenic differentiation and function.⁴¹

A recent study has demonstrated the hormetic-like concentration-dependent response of resveratrol and other natural compounds inducing biologically reverse effects at different doses.¹⁷ The nature of pro-oxidant or antioxidant of the candidates depends on their concentrations and pH, that could play a pivotal role in cell growth and survival.⁴² Autophagy is also crucial in maintaining bone homeostasis through degradation of osteoclasts, osteoblasts and osteocytes. Autophagy is a stress-response mechanism for cell survival and a homeostatic process based on lysosome-dependent intracellular degradation system.⁴³ In an earlier study, adenosine monophosphate-activated protein kinase (AMPK), a heterotrimeric protein kinase, has been shown to regulate osteogenic differentiation of human mesenchymal stem cells by early mTOR inhibition-mediated autophagy and late activation of the Akt/mTOR signaling axis.⁴⁴ Phytomolecules have played potential correlation between autophagy and bone pathogenesis. In a previous study, resveratrol accelerated osteogenic differentiation in differentiating of human gingival mesenchymal stem cells via activating AMPK-BECLIN-1 pro-autophagic pathway.⁴⁵ In addition, kaempferol, a flavonol, promoted the osteogenic differentiation of cultured MC3T3-E1 osteoblast cells by inducing autophagy at low concentration, however, it showed cytotoxic effect at higher

concentration.⁴⁶ Interestingly, our study also demonstrated that MO acted as cytotoxic agent at high concentration, however, low concentration induced the cell proliferation.

In addition, an *in silico* molecular docking analysis was conducted to investigate the binding interaction of potential components of MOL β -sitosterol, quercetin, and kaempferol with BMP2 and Runx-2 proteins through AutoDock Vina and iGEMDOCK 2.1 tools. Interestingly, all the active components of MOL exhibited good binding affinity with BMP2 and Runx2 proteins. The molecular interactions represent interacting residues in binding pockets with specific physico-chemical properties which indicate specific functions of the target protein.⁴⁷ This result suggested that interacting amino acids with ligand molecules were attached with H-bond, alkyl, pi-alkyl, and van der Waals forces which stabilized the complex structure.⁴⁸ The calculated values of various physicochemical parameters of the selected compounds for drug likeness by applying Lipinski's rule of five are shown in Table 3. The violation performed by Lipinski should not be more than one for an orally active medicine.⁴⁹ Interestingly, there were no violations of Lipinski's rule of five in any of the active components. Furthermore, drug absorption % refers to the amount of drug absorbed from the gastrointestinal lumen into the blood of the hepatic portal vein.⁵⁰ Table 3 shows that the highest percentage of β -sitosterol was absorbed orally, followed by kaempferol, and finally quercetin. As analysed by OSIRIS Data Warrior V5.2.1 software, β -sitosterol was found to be druglikeness and non-toxicity characteristics, followed by kaempferol and quercetin (Table 4). The bioactivity score is an important indicator of a biomolecule's potency. The greater the bioactivity score, the more probable the component is to be active.²⁶ As it is cleared from Table 5, β -sitosterol was found to be biologically active components against GPCR and acting as ion channel modulator, nuclear receptor, protease inhibitor and enzyme inhibitor. Quercetin and kaempferol, on the other hand, showed active kinase and other enzyme inhibitors and act as active components against nuclear receptor. The absorption, distribution, metabolism, excretion, and toxicity features of the components were also calculated using the online SwissADME software to determine their pharmacokinetics (Table 6). All components were shown to be lipid soluble, indicating good absorption over skin, as determined by the LogP value. The ATP-dependent bioavailability protein pump permeability-glycoprotein (P-gp) removes medicines from biological systems. Interestingly, neither of the phytocomponents showed BBB permeability nor were they predicted to behave as P-gp substrates. Cytochrome P450 (CYPs) is a family of important metabolic enzymes that serve in the biotransformation of xenobiotics in order to protect tissues. Furthermore, only the CYP1A2, CYP2D6, and CYP3A4 isoenzymes of the CYP family interacted with quercetin and kaempferol among the three phytocomponents studied, providing its efficiency with little toxicity. The current *in vitro* and *in silico* investigations have demonstrated a hormetic-like biphasic dose response of MOL on bone cells proliferation and differentiation, which may impart dose-dependent efficacy of MOL in clinical study of the health sector.

5. Conclusion

This study demonstrated that MO worked as anti-osteosarcoma agent at high concentration *via* modulating ROS, chromatin condensation, and cell cycle arrest. Low concentrations, on the other hand, stimulated proliferation, differentiation, and mineralization and expression level of BMP2 and Runx2 genes. Thus, hormetic-like biphasic concentration-dependent response of MOL might be crucial element in bone pathogenesis. Although this is a preliminary study, few limitations of this study could be resolved by examining the expression level of BMP2 and Runx2 proteins at

various concentrations of MOL as well as the mechanisms underlying osteogenic-like differentiation of SaOS2 cells. This study also necessitates further a preclinical investigation to determine its efficient and safe dosages in prospective drug development.

Financial Support

None.

Author contributions

MIK and SS performed the experiments. SS, MIK, MAB, FSA, FA, HAB, AAA, and MA were involved in designing the experiments. MAB, HAB, and MA helped with statistical analysis. The final manuscript was read and approved by all contributors.

Data availability

All data are available in the manuscript.

Declaration of competing interest

The authors declare no conflicts of interest.

Acknowledgments

The authors extend their appreciation to the Deputyship for Research & Innovation, Ministry of Education, Saudi Arabia for funding research work through the project number (QU-IF-2-2-2-27064). The authors also thank Qassim University for technical support. The flow cytometry facility was provided by SAIF-Division, CSIR-CDRI. Sahabjada Siddiqui expresses his gratitude to the Department of Biochemistry at Era's Lucknow Medical College & Hospital, Era University, Lucknow, India, for providing cell culture facilities.

References

- Curtis EM, Dennison EM, Cooper C, Harvey NC. Osteoporosis in 2022: care gaps to screening and personalised medicine. *Best Pract Res Clin Rheumatol*. 2022 Jun 9, 101754.
- Johnell O, Kanis JA. An estimate of the worldwide prevalence and disability associated with osteoporotic fractures. *Osteoporos Int*. 2006;17(12):1726–1733.
- Adami G, Fassio A, Gatti D, et al. Osteoporosis in 10 years time: a glimpse into the future of osteoporosis. *Therapeutic Advances in Musculoskeletal Disease*. 2022 Mar;14, 1759720X221083541.
- Ström O, Borgström F, Kanis JA, et al. Osteoporosis: burden, health care provision and opportunities in the EU. *Arch. Osteoporos*. 2011 Dec;6(1):59–155.
- Tabish SA. Complementary and alternative healthcare: is it evidence-based? *Int J Health Sci*. 2008 Jan;2(1). V-IX. PMID: 21475465; PMCID: PMC3068720.
- Atanasov AG, Waltenberger B, Pferschy-Wenzig EM, et al. Discovery and resupply of pharmacologically active plant-derived natural products: a review. *Biotechnol Adv*. 2015 Dec;33(8):1582–1614.
- Siddiqui S, Khatoun A, Ahmad K, et al. Traditional Islamic herbal medicine and complementary therapies. In: Bernardo-Filho M, Tair R, De Sá-Caputo DC, Seixas A, eds. *Complementary Therapies [Working Title]*. IntechOpen; 2022. <https://doi.org/10.5772/intechopen.101927>.
- Swamy MK, Patra JK, Rudramurthy GR, eds. *Medicinal Plants: Chemistry, Pharmacology, and Therapeutic Applications*. CRC Press; 2019 May 10.
- Anwar F, Latif S, Ashraf M, Gilani AH. Moringa oleifera: a food plant with multiple medicinal uses. *Phytother Res*. 2007 Jan;21(1):17–25.
- Abdull Razis AF, Ibrahim MD, Kntayya SB. Health benefits of Moringa oleifera. *Asian Pac J Cancer Prev APJCP*. 2014;15(20):8571–8576.
- Meireles D, Gomes J, Lopes L, Hinzmann M, Machado J. A review of properties, nutritional and pharmaceutical applications of Moringa oleifera: integrative approach on conventional and traditional Asian medicine. *Adv Tradit Med*. 2020 Aug;17:1–21.
- Paikra BK, Khongde HKJ, Gidwani B. Phytochemistry and pharmacology of *Moringa oleifera* Lam. *J Pharmacopuncture*. 2017 Sep;20(3):194–200.
- Singh V, Singh N, Pal US, Dhasmana S, Mohammad S, Singh N. Clinical evaluation of cissus quadrangularis and moringa oleifera and osteosarcoma as osteogenic agents in mandibular fracture. *Natl J Maxillofac Surg*. 2011 Jul;2(2):132–136.

14. Bhattacharya A, Tiwari P, Sahu PK, Kumar S. A review of the phytochemical and pharmacological characteristics of *Moringa oleifera*. *J Pharm BioAllied Sci*. 2018 Oct-Dec;10(4):181–191.
15. Vergara-Jimenez M, Almatrafi MM, Fernandez ML. Bioactive components in moringa oleifera leaves protect against chronic disease. *Antioxidants*. 2017 Nov 16;6(4):91.
16. Saleem A, Saleem M, Akhtar MF, Ashraf Baig MMF, Rasul A. HPLC analysis, cytotoxicity, and safety study of *Moringa oleifera* Lam. (wild type) leaf extract. *J Food Biochem*. 2020 Jul 29, e13400.
17. Jodynis-Liebert J, Kujawska M. Biphasic dose-response induced by phytochemicals: experimental evidence. *J Clin Med*. 2020 Mar 6;9(3):718.
18. Rietjens IMCM, Louisse J, Beekmann K. The potential health effects of dietary phytoestrogens. *Br J Pharmacol*. 2017 Jun;174(11):1263–1280.
19. Ying C, Hsu JT, Hung HC, Lin DH, Chen LF, Wang LK. Growth and cell cycle regulation by isoflavones in human breast carcinoma cells. *Reprod Nutr Dev*. 2002 Jan-Feb;42(1):55–64.
20. Maggiolini M, Bonfiglio D, Marsico S, et al. Estrogen receptor alpha mediates the proliferative but not the cytotoxic dose-dependent effects of two major phytoestrogens on human breast cancer cells. *Mol Pharmacol*. 2001 Sep;60(3):595–602. PMID: 11502892.
21. Siddiqui S, Arshad M. Osteogenic potential of punica granatum through matrix mineralization, cell cycle progression and runx2 gene expression in primary rat osteoblasts. *Daru*. 2014 Nov 20;22(1):72.
22. Siddiqui S, Mahdi AA, Arshad M. Genistein contributes to cell cycle progression and regulates oxidative stress in primary culture of osteoblasts along with osteoclasts attenuation. *BMC Compl Med Ther*. 2020 Sep 11;20(1):277.
23. Arumugam A, Ibrahim MD, Kntayya SB, et al. Induction of apoptosis by gluconasturtiin-Isothiocyanate (GNST-ITC) in human hepatocarcinoma HepG2 cells and human breast adenocarcinoma MCF-7 cells. *Molecules*. 2020 Mar 9;25(5):1240.
24. Lin JH, Deng LX, Wu ZY, Chen L, Zhang L. Pilose antler polypeptides promote chondrocyte proliferation via the tyrosine kinase signaling pathway. *J Occup Med Toxicol*. 2011 Nov 10;6:27.
25. Siddiqui S, Upadhyay S, Ahmad R, et al. Virtual screening of phytoconstituents from miracle herb *nigella sativa* targeting nucleocapsid protein and papain-like protease of SARS-CoV-2 for COVID-19 treatment. *J Biomol Struct Dyn*. 2020 Dec 8:1–21.
26. Khan T, Ahmad R, Azad I, Raza S, Joshi S, Khan AR. Computer-aided drug design and virtual screening of targeted combinatorial libraries of mixed-ligand transition metal complexes of 2-butanone thiosemicarbazone. *Comput Biol Chem*. 2018 Aug;75:178–195.
27. Lipinski CA. Lead- and drug-like compounds: the rule-of-five revolution. *Drug Discov Today Technol*. 2004 Dec;1(4):337–341.
28. Wu F, Zhou Y, Li L, et al. Computational approaches in preclinical studies on drug discovery and development. *Front Chem*. 2020 Sep 11;8:726.
29. Daina A, Michielin O, Zoete V. SwissADME: a free web tool to evaluate pharmacokinetics, drug-likeness and medicinal chemistry friendliness of small molecules. *Sci Rep*. 2017 Mar 3;7, 42717.
30. Setiawati R, Rahardjo P. *Bone Development and Growth. Osteogenesis and Bone Regeneration*. 2019 Apr 24:10.
31. Abiramasundari G, Sumalatha KR, Sreepriya M. Effects of *Tinospora cordifolia* (Menispermaceae) on the proliferation, osteogenic differentiation and mineralization of osteoblast model systems in vitro. *J Ethnopharmacol*. 2012 May 7;141(1):474–480.
32. Bhargavan B, Gautam AK, Singh D, et al. Methoxylated isoflavones, cajanin and isoformononetin, have non-estrogenic bone forming effect via differential mitogen activated protein kinase (MAPK) signaling. *J Cell Biochem*. 2009 Oct 1;108(2):388–399.
33. Chauhan S, Sharma A, Upadhyay NK, Singh G, Lal UR, Goyal R. In-vitro osteoblast proliferation and in-vivo anti-osteoporotic activity of *Bombax ceiba* with quantification of Lupeol, gallic acid and β -sitosterol by HPTLC and HPLC. *BMC Compl Alternative Med*. 2018 Aug 7;18(1):233.
34. Jung IL, Lee JH, Kang SC. A potential oral anticancer drug candidate, *Moringa oleifera* leaf extract, induces the apoptosis of human hepatocellular carcinoma cells. *Oncol Lett*. 2015 Sep;10(3):1597–1604.
35. Abbasi N, Khosravi A, Aidi A, Shafiei M. Biphasic response to luteolin in MG-63 osteoblast-like cells under high glucose-induced oxidative stress. *Iran J Med Sci*. 2016 Mar;41(2):118–125.
36. Berndt K, Campanile C, Muff R, Strehler E, Born W, Fuchs B. Evaluation of quercetin as a potential drug in osteosarcoma treatment. *Anticancer Res*. 2013 Apr;33(4):1297–1306. PMID: 23564766.
37. Zhang X, Feng H, Du J, et al. Aspirin promotes apoptosis and inhibits proliferation by blocking G0/G1 into S phase in rheumatoid arthritis fibroblast-like synoviocytes via downregulation of JAK/STAT3 and NF- κ B signaling pathway. *Int J Mol Med*. 2018 Dec;42(6):3135–3148.
38. Aubin JE, Liu F, Malaval L, Gupta AK. Osteoblast and chondroblast differentiation. *Bone*. 1995 Aug;17(2 Suppl):77S–83S.
39. Matsubara T, Kida K, Yamaguchi A, et al. BMP2 regulates Osterix through *Msx2* and *Runx2* during osteoblast differentiation. *J Biol Chem*. 2008 Oct 24;283(43):29119–29125.
40. Liu TM, Lee EH. Transcriptional regulatory cascades in *Runx2*-dependent bone development. *Tissue Eng B Rev*. 2013 Jun;19(3):254–263.
41. Braveboy-Wagner J, Sharoni Y, Lelkes PI. Nutraceuticals synergistically promote osteogenesis in cultured 7F2 osteoblasts and mitigate inhibition of differentiation and maturation in simulated microgravity. *Int J Mol Sci*. 2021 Dec 23;23(1):136. <https://doi.org/10.3390/ijms23010136>. PMID: 35008559; PMCID: PMC8745420.
42. Bouayed J, Bohn T. Exogenous antioxidants—Double-edged swords in cellular redox state: health beneficial effects at physiologic doses versus deleterious effects at high doses. *Oxid Med Cell Longev*. 2010 Jul-Aug;3(4):228–237.
43. Das G, Shrivastava BV, Baehrecke EH. Regulation and function of autophagy during cell survival and cell death. *Cold Spring Harbor Perspect Biol*. 2012 Jun 1;4(6), a008813.
44. Pantovic A, Krstic A, Janjetovic K, et al. Coordinated time-dependent modulation of AMPK/Akt/mTOR signaling and autophagy controls osteogenic differentiation of human mesenchymal stem cells. *Bone*. 2013 Jan;52(1):524–531.
45. Vidoni C, Ferraresi A, Secomandi E, et al. Autophagy drives osteogenic differentiation of human gingival mesenchymal stem cells. *Cell Commun Signal*. 2019 Aug 19;17(1):98. <https://doi.org/10.1186/s12964-019-0414-7>. PMID: 31426798; PMCID: PMC6701103.
46. Kim IR, Kim SE, Baek HS, et al. The role of kaempferol-induced autophagy on differentiation and mineralization of osteoblastic MC3T3-E1 cells. *BMC Compl Alternative Med*. 2016 Aug 31;16(1):333. <https://doi.org/10.1186/s12906-016-1320-9>. PMID: 27581091; PMCID: PMC5007678.
47. Korkuć P, Walther D. Physicochemical characteristics of structurally determined metabolite-protein and drug-protein binding events with respect to binding specificity. *Front Mol Biosci*. 2015 Sep 15;2:51.
48. Brylinski M. Aromatic interactions at the ligand-protein interface: implications for the development of docking scoring functions. *Chem Biol Drug Des*. 2018 Feb;91(2):380–390.
49. Benet LZ, Hosey CM, Ursu O, Oprea TI. BDDCS, the Rule of 5 and drugability. *Adv Drug Deliv Rev*. 2016 Jun 1;101:89–98.
50. van de Waterbeemd H. Physicochemical properties in drug profiling. *Methods Princ Med Chem*. 2008:25–52.